 doi:10.1111/j.1471-4159.2006.04344.x

Early gene expression during natural spinal cord regeneration in the salamander *Ambystoma mexicanum*

James R. Monaghan,* John A. Walker,* Robert B. Page,* Srikrishna Putta,* Christopher K. Beachy† and S. Randal Voss*

**Department of Biology & Spinal Cord and Brain Injury Research Center, University of Kentucky, Lexington, Kentucky, USA*
†*Department of Biology, Minot State University, Minot, North Dakota, USA*

Abstract

In contrast to mammals, salamanders have a remarkable ability to regenerate their spinal cord and recover full movement and function after tail amputation. To identify genes that may be associated with this greater regenerative ability, we designed an oligonucleotide microarray and profiled early gene expression during natural spinal cord regeneration in *Ambystoma mexicanum*. We sampled tissue at five early time points after tail amputation and identified genes that registered significant changes in mRNA abundance during the first 7 days of regeneration. A list of 1036 statistically significant genes was identified. Additional statistical and fold change criteria were applied to identify a smaller list of 360 genes that were used to describe predominant expression patterns and gene functions. Our results show that a diverse injury response is activated in concert with extracellular matrix remodeling mechanisms during the early acute phase of natural spinal cord regeneration. We also report gene expression similarities and differences between our study and studies that have profiled gene expression after spinal cord injury in rat. Our study illustrates the utility of a salamander model for identifying genes and gene functions that may enhance regenerative ability in mammals.

Keywords: axolotl, *in situ* hybridization, microarray, regeneration, salamander, spinal cord.
J. Neurochem. (2007) 10.1111/j.1471-4159.2006.04344.x

Salamanders have a remarkable ability to regenerate complex body parts including the limb, tail, lens, and CNS. Although salamander regeneration has been studied for several hundred years (Spallanzani 1768; Müller 1864), molecular-level studies have been limited to a relatively few important transcription factors and signaling molecules that are highly conserved among vertebrates, and in some cases metazoans (e.g., Schnapp *et al.* 2005; Christensen *et al.* 2002; Carlson *et al.* 2001; Caubit *et al.* 1997; Torok *et al.* 1999). Broader assessments of gene expression during salamander regeneration may identify mechanisms that can be exploited to enhance regenerative ability in humans.

Salamanders regenerate their spinal cords and regain full movement and function after tail amputation. Within a few hours of amputation, injury responses are initiated to increase cell survival and transform the tissue-damaged environment into one that is permissive for repair and subsequent regeneration. It is possible that the unrivaled regenerative ability of salamanders is due in part to this early injury response phase of regeneration, but very little is known about early response genes and associated biological processes. Most attention has been directed to understand cellular and developmental changes during the dramatic and conspicuous de-differentiation and re-patterning phases of regeneration. During de-differentiation, cells of mesodermal origin (muscle, dermal fibroblasts, and cartilage) re-enter the cell cycle and proliferate to form a mass called the blastema (Hay and Fischman 1961). Blastemal cells subsequently re-differentiate into mesodermal tissues but apparently do not contribute to the regenerating spinal cord. Epithelial cells (ependymoglia) of the ependymal lining that surrounds the central canal

Received July 11, 2006; revised manuscript received August 24, 2006; accepted September 17, 2006.

Address correspondence and reprint requests to S. Randal Voss Ph. D., 741 South Limestone Avenue, Lexington, KY 40536, USA.
E-mail: srvoss@uky.edu

Abbreviations used: apoE, apolipoprotein E; BMP, bone morphogenic protein; C, constant; ck18, cytokeratin 18; d, day; D, down-regulated; DIG, digoxygenin; ECM, extracellular matrix; EST, expressed sequence tag; FDR, false discovery rate; FGF, fibroblast growth factor; fst, follistatin; FWER, family-wise error rate; ISH, *in situ* hybridization; lgals1, galectin 1; mmp, matrix metalloproteinase; N, non-significant; PCA, principal component analysis; QRT-PCR, quantitative real-time PCR; sfrp2, secreted frizzled-related protein 2; SHH, sonic hedgehog; U, up-regulated.

of the spinal cord re-form neural tissues of the regenerating spinal cord (Nordlander and Singer 1978). The signals that initiate and maintain the proliferative response of ependymoglia are largely unknown, however, recent studies implicate some of the same highly conserved genes that are known to regulate the proliferation and differentiation of neural stem cells among vertebrates (O'Hara and Chernoff 1994; Zhang *et al.* 2000, 2002; Schnapp *et al.* 2005). This suggests that some aspects of salamander spinal cord regeneration may be shared with organisms that have little or no potential for neural regeneration. Analyses of gene expression in salamanders may point to key similarities and differences that are associated with regenerative ability.

We designed a custom Affymetrix GeneChip and performed the first microarray analysis of spinal cord regeneration in the Mexican axolotl (*Ambystoma mexicanum*). We sampled regenerating spinal cord tissue at five early time points after amputation and identified differentially expressed genes and temporal patterns of gene expression. We compared our lists of significantly regulated genes to lists that have been similarly compiled from microarray studies of spinal cord injury in rat. Our results highlight genes and gene expression patterns that are associated with the salamander's natural ability to regenerate spinal cord.

Materials and methods

Animals, tissue collection, and RNA isolation

The handling and surgical manipulation of all salamanders was carried out according to the University of Kentucky Animal Care and Use guidelines (IACUC #00609L2003). The caudal 1/3 of the tail was amputated from 225 Mexican axolotl sibs (*mean snout-vent length* = 6.2 cm) from an inbred Voss laboratory strain. Spinal cord tissue was collected 1.0 mm rostral to the injury plane at the time of spinal cord transection (day 0), and also on 1, 3, 5, and 7 days post-amputation. The tail blastema was removed prior to sampling, however, it is likely that some infiltrating blastemal cells were represented in the day 1–7 samples. Total RNA (*mean* = 1.7 μg) was extracted from pools of nine tissues for each of five replicates that were collected at each time point. Probe labeling, hybridization, and scanning for the 25 RNA samples were performed by a single staff member of the University of Kentucky Microarray Core Facility.

Development of a microarray platform

A custom *Ambystoma* Affymetrix GeneChip was designed from curated expressed sequence tag (EST)s assemblies for *A. mexicanum* and *A. t. tigrinum* as described in Page *et al.* (2006). These ESTs are enriched for genes expressed in neural and regenerating tissues (Putta *et al.* 2004). Briefly, the array contains 4844 total probe sets, 254 of which are controls or replicate probe sets. Of the remaining 4590 probe sets, all but 188 correspond to unique *A. mexicanum* contigs, of which 2960 are significantly identical in nucleotide composition (e-7; BLASTX) to a human sequence in the non-redundant, RefSeq protein database. Significant salamander–human blast hits were considered gene orthologs in our analyses and we assumed that salamander–human orthologs have similar gene functions or ontologies. Raw data files can be obtained at http://www.ambystoma.org.

Quality control and low level analyses

We used the Bioconductor package affy (http://www.bioconductor.org) that is available for the statistical programming environment R (http://www.r-project.org) to perform quality control and pre-processing procedures at the individual probe level (Bolstad *et al.* 2005a). These procedures included: (i) generating matrices of M versus A plots for all replicate arrays; (ii) investigating measures of central tendency, measures of dispersion, and the distributions of all 25 arrays via boxplots and histograms; (iii) viewing images of the $\log_2$ (intensity) values for each array to check for spatial artifacts; and (iv) viewing an RNA degradation plot (Bolstad *et al.* 2005b) that allows for visualization of the 3′ RNA labeling bias across all arrays simultaneously. In addition, we used ArrayAssist Lite software (Stratagene, La Jolla, CA, USA) and the MAS5.0 algorithm to assess several quality control measures that are recommended by Affymetrix (http://www.affymetrix.com), such as average background (mean = 61.5, range = 55–81.5), noise (mean = 4.23, range = 2.89–6.94), and percent present (mean = 84.7% range = 81.2–87.0%). This high number of present probe sets likely reflects the biased selection of regeneration-associated genes and high quality contigs for probe set design. Next, the repeatability of probe set estimates of hybridization intensity was evaluated between arrays. We examined the correlation of hybridization intensities across all probe sets among the biological replicates for each regeneration time point (mean $r = 0.994$; range $r = 0.983$–0.998). These results demonstrate that we were able to obtain a high level of repeatability. We processed our data similarly to the methods of Choe *et al.* (2005) to determine a probe set intensity value. Briefly, our processing method consisted of using the MAS 5.0 background correction algorithm, the quantiles algorithm for probe-level normalization, the MAS 5.0 algorithm for perfect match/mismatch correction, the median polish algorithm for expression summary generation, and a loess normalization at the probe set level using the GoldenSpike package for R (Choe *et al.* 2005; http://www.ccr.buffalo.edu/halfon/spike/index.html).

Detection of differentially expressed genes and data filtration

Microarray platforms may not accurately or precisely quantify genes with low intensity values (Choe *et al.* 2005; Draghici *et al.* 2006). Because low intensity genes contribute to the multiple testing problem that is inherent to all microarray studies, we filtered 1203 probe sets whose mean intensity across all 25 arrays were smaller than or equal to the mean of the lowest quartiles across all arrays (*mean* = 6.44, *SD* = 0.09; data presented on a $\log_2$ scale). Probe sets (3641) were then tested for differential expression via a one-way fixed effect linear model (intensity = day sampled) using the F_s-test of Cui *et al.* (2005) and J/MAANOVA software (http://www.jax.org/staff/churchill/labsite/software/ANOVA/index.html). Initially, we adjusted for multiple testing by setting the false discovery rate (FDR) to 0.01 using the step-up algorithm of Benjamini and Hochberg (1995). As is shown in Fig. 1a, upon performing this FDR correction, 2771 probe sets of the 3641 probe sets tested (76.11%) were selected as differentially expressed. We then took a more

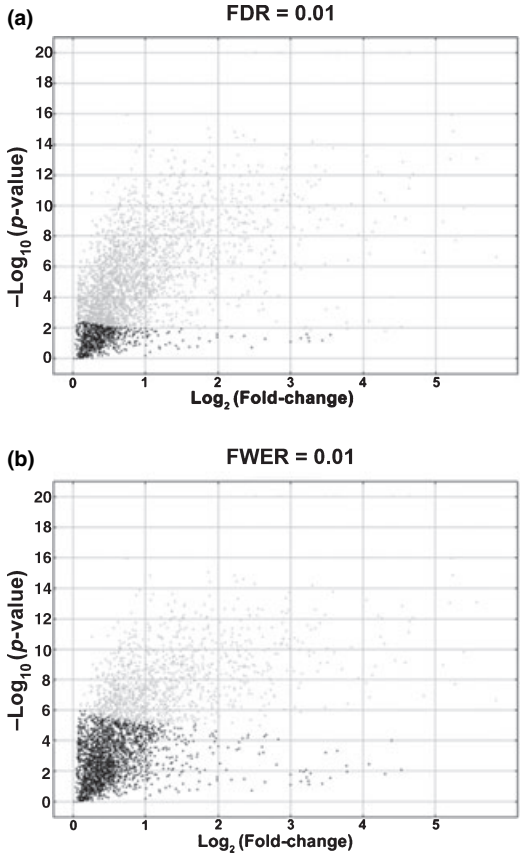

Fig. 1 Volcano plots showing the number of genes selected as differentially expressed with the FDR set to 0.01 (a) and the FWER set to 0.01 (b). Genes selected by each of these respective criteria are gray and non-selected genes are black.

conservative approach to our first pass at selecting differentially expressed genes by setting the family-wise error rate (FWER) to 0.01. Upon adjusting the FWER to 0.01, 1273 of the 3641 genes tested (34.96%) were selected as differentially expressed (Fig. 1b). In order to identify a smaller subset of probe sets, we prioritized probe sets that were selected as differentially expressed that exhibited: (i) a twofold change at any time point relative to day 0 and (ii) F_s-values that were in the upper 50% of these 1273 genes ($F_s > 28.36$), leading to a total of 376 probe sets. The intensity values of three probe sets pairs designed for the same contigs, as well as probe sets corresponding to the same human gene were combined, yielding a final short list of 360 unique genes (Table 1; Table S1).

Candidate gene lists may differ when different preprocessing algorithms are used to identify statistically significant genes from oligonucleotide microarrays (Millenaar *et al.* 2006). To address this concern, we compared the 376 candidate probe set list above to a 646 probe set list that was generated using only the robust Robust-Multiarray Averaging algorithm (Irizarry *et al.* 2003), One-way ANOVA (FDR = 0.01), and a twofold change criterion. Only 11 of the 376 candidate probe sets (2.9%) were unique, indicating that our methodology for identifying candidate genes is largely concordant with other statistical approaches.

Identification of gene expression patterns

We used the following criteria to define temporal gene expression patterns for the 360 genes that met statistical and fold-level criteria. For each gene we assigned a score to qualify the mRNA abundance at each post-amputation sample time (d1, d3, d5, and d7). A gene received a score of non-significant (N) for each sample time that mRNA abundance was <2-fold deviant of the d0 estimate. We refer to the d0 estimate as the baseline estimate of mRNA abundance. A gene received a score of up-regulated (U) or down-regulated (D) for the first post-amputation sample time that mRNA abundance deviated by ≥2-fold from baseline. For subsequent sample times, each gene received one of three possible scores: C, U, or D. A score of constant (C) was assigned if the fold level estimate was <2-fold deviant of the previous U or D estimate (C was never assigned after N), and ≥2-fold deviant from baseline. A score of U or D was assigned if mRNA abundance deviated again by ≥2-fold. Using this scoring system, a gene received a score of U, D, or N for d1, and U, D, N, or C for d3, 5, and 7. A complete breakdown of the 360 changed genes is shown in Table S2. To annotate genes, we used multiple databases (GO, KEGG, IHOP, OMIM, etc.) and searched the literature for information about the expression and functions of each gene that we identified as significant in our study. We biased our annotations to emphasize possible gene functions that have been described in regeneration and spinal cord injury research fields.

Identification of genes expressed differently in salamander tail regeneration and rat spinal cord injury

A bioinformatics approach was used to identify gene orthologs that are expressed similarly or differently after salamander tail amputation versus rat spinal cord injury. We used current (as of May 2006) human Entrez Gene IDs that were assigned to each annotated probe set on the *Ambystoma* GeneChip to identify all presumptive salamander orthologs on RatU34A, B, and C GeneChips. To accomplish this cross-referencing task, we used Resourcerer (Tsai *et al.* 2001), a database that allows orthologous genes to be identified among species-specific microarray resources. This yielded a list of 1036 probe sets between the *Ambystoma* and RatU34 GeneChips that presumably correspond to 662 unique, orthologous genes. We compared the expression pattern of each of these genes using results from this study and published studies that profiled gene expression after SCI in rat, using RatU34 GeneChips (Carmel *et al.* 2001; Song *et al.* 2001; Aimone *et al.* 2004; De Biase *et al.* 2005). De Biase *et al.* (2005) provide a table that compares specific details of these rat SCI microarray studies. The rat studies used thoracic T8-10 contusion models (MASCIS, OSU, and weight drop methods) and tissues were sampled at and flanking the impact site during the first 48 h post-injury; Aimone *et al.* (2004) also sampled 7 and 35 days after injury. For each gene, we qualified gene expression as either significantly up, significantly down, or non-significant. We used statistical and fold-level criteria (FWER <0.01; >2-fold change) to score salamander genes for these criteria. If a gene was reported as significantly regulated in the rat studies, we recorded it as such; otherwise, we recorded it as non-significant.

Quantitative real-time PCR

Ten genes from the microarray experiment were selected for validation by quantitative real-time PCR (QRT-PCR). Genes were

Table 1 Gene symbols and functions for 360 changed salamander genes during the first week of spinal cord regeneration

Symbol	Function	Symbol	Function
UCCC = 64	**Unk; *n* = *30***	PAICS	Purine metabolism
MYO1B	Actin binding	CTPS	Pyrimidine biosynthesis
TAGLN	Actin binding	SSB	mRNA processing
ADFP	Lipid metabolism	EXOSC2	rRNA processing
TNFAIP8	Anti-apoptotic	RANBP1	Signal transduction
ETHE1	Anti-apoptotic	TPRT	Ubiquinone biosynthesis
LGALS1	Apoptosis	C6ORF115	Unknown
GADD45G	Apoptosis	CCDC58	Unknown
GADD45B	Apoptosis	**NNDC = 27**	**Unk; *n* = *8***
EFHD2	Calcium binding	CDKN1C	Negative cell proliferation
AGC1	Unknown	MLF1	Cell differentiation
MYC	Cell cycle	KRT6L	Cytoskeleton
CTSL	Cysteine protease	ABLIM1	Cytoskeleton
CTSK	Cysteine protease	GLUD1	Glutamate catabolism
TUBB6	Cytoskeleton	ATP1B3	Ion transport
FBP1	Glycolysis	FXYD3	Ion transport
B3GNT5	Glycosylation	PRKAG2	Lipid metabolism
TGFB1	Growth factor	COX4I2	Metabolism
TYROBP	Immune response	BHMT	Metabolism
SLC11A1	Immune response	PCBD	Metabolism
MPEG1	Immune response	CKMT1A	Metabolism
CXCR4	Immune response	SERPINI1	Neurogenesis
LGALS3BP	Immune response	ABAT	Neurotransmission
CYBB	Immune response	TM4SF2	Protein biosynthesis
ANKRD1	Injury response	GNB5	Signal transduction
FTH1	Iron homeostasis	POLR2L	Transcription
ATP6V0D1	Proton transport	C6ORF110	Unknown
C1ORF33	Ribosomal	FAM79A	Unknown
MAP2K3	Signal transduction	**NUCC = 24**	**Unk; *n* = *6***
MMP9	Tissue remodeling	TAGLN	Actin binding
MMP1	Tissue remodeling	ASAH1	Apoptosis
LYN	Tyrosine kinase	UHRF1	Cell cycle; S
TMEM49	Unknown	CDK4	Cell cycle; G1/S
FLJ2262	Unknown	KIAA0101	Cell cycle; S
WNT5A	WNT signaling	PPGB	Cellular transport
NNUC = 44	**Unk; *n* = *14***	LGMN	Cysteine protease
GLRX	Antioxidant	CSTB	Protease inhibitor
LGALS3	Carbohydrate binding	RRM2	DNA metabolism
KIF11	Cell cycle; M	ANXA1	Inflammation
CCNB3	cell cycle; G2/M	THBS2	ECM component
PLK1	Cell cycle; G1/S: G2/M	GLB1	Metabolism
RFC2	Cell cycle; S	ATP6V0E	Proton transport
PCNA	Cell cycle; S	RPL31	Ribosomal
MCM7	Cell cycle; S	APOE	Lipid metabolism
STK6	Cell cycle; M	METTL2	Ubiquinone biosynthesis
CCNA2	Cell cycle; G1/S: G2/M	CCDC43	Unknown
CDC2	Cell cycle; G1/S: G2/M	ANGPTL2	Growth factor
CHEK1	Cell cycle; DNA damage	**UNNN = 20**	**Unk; *n* = *7***
MAD2L1	Cell cycle; M	BYSL	Cell adhesion
CDC20	Cell cycle; M	GLN3	Cell cycle; G1/S
AURKB	Cell cycle; M	DUSP1	Heat shock
CDCA8	Cell cycle; M	IRF1	Immune response
KRT18	Cytoskeleton	HSPA5	Injury response
CALD1	Cytoskeleton	SLC30A1	Ion transport
FEN1	DNA metabolism	AGXT2L1	Metabolism
SLBP	mRNA processing	DKC1	Ribosomal

Table 1 Continued

Symbol	Function	Symbol	Function
CKAP4	Inflammation	RPS6KA1	Signal transduction
KPNA2	Intracellular transport	PUS1	tRNA processing
VRK1	Kinase	FLJ36031	Unknown
COL12A1	ECM component	TGM1	Injury response
UCP2	Neuroprotection	IFIH1	Immune response
CTSK	Protease	**UUCC = 12**	**Unk; *n* = *8***
OLFML2B	Signal transduction	F13A1	Wound healing
CNIH4	Unknown	MARCO	Immune response
CCDC82	Unknown	FABP2	Lipid metabolism
RPL38	Ribosomal	GPNMB	Negative cell proliferation
NDCC = 42	**Unk; *n* = *22***	**UDCC = 10**	**Unk; *n* = *6***
KRT7	Cytoskeleton	TFPI2	Coagulation
KIF21A	Cytoskeleton	MMP1	Tissue remodeling
SLC1A2	Glutamate transport	GIF	Vitamin B transport
SLC1A3	Glutamate transport	C8ORF4	WNT signaling
HSPA8	Heat shock	**UCDC = 8**	**Unk; *n* = *3***
TTR	Hormone transport	HMOX1	Heat shock
SLC12A2	Ion transport	MMP13	Tissue remodeling
KCTD3	Ion transport	MMP1	Tissue remodeling
FDPS	Lipid metabolism	TIMP1	Tissue remodeling
FAAH	Lipid metabolism	JUNB	Transcription
COL8A1	ECM component	**DCCC = 6**	**Unk; *n* = *5***
FBN2	ECM component	CYP2A13	Metabolism
GSTM4	Metabolism	**UCCN = 4**	
GRM3	Neurotransmission	LTB4DH	Antioxidant
PADI3	Protein metabolism	TXNDC2	Antioxidant
APCDD1	Signal transduction	TXN	Antioxidant
TJP1	Signal transduction	BTBD3	Protein binding
APC	Signal transduction	**DCNN = 4**	**Unk; *n* = *2***
MAPRE3	Structural protein	RGMA	Axon guidance
CRYAB	Structural protein	FHL1	Protein binding
NNND = 35	**Unk; *n* = *17***	**UCNN = 5**	
PDCD4	Apoptosis	CES1	Neuroprotection
APP	Apoptosis	USP2	Protein breakdown
CCNI	Cell cycle	RAP2B	Signal transduction
SPTAN1	Cytoskeleton	SAT	Polyamine homeostasis
SPTBN1	Cytoskeleton	CD63	Signal transduction
PYGM	Glycogen metabolism	**UNNU = 3**	**Unk; *n* = *2***
FABP7	Lipid metabolism	NOL5A	Ribosomal
CHPT1	Lipid metabolism	**NUCN = 3**	
SLC25A4	Mitochondrial transport	HRAS	Cell proliferation
GPM6B	Neurogenesis	NSUN2	Cell proliferation
AHNAK	Neurogenesis	LTBP1	TGF-beta signaling
GSTM1	Neuroprotection	**UNND = 3**	**Unk; *n* = *3***
GSTP1	Neuroprotection	**NNUU = 2**	
GABARAPL2	Neurotransmission	COL11A1	ECM component
PBP	Protease inhibitor	POSTN	Skeletal development
CALCA	Signal transduction	**NUNN = 2**	**Unk; *n* = *2***
TRAPPC6B	Transport	**UNUC = 2**	**Unk = 2**
C11ORF74	Unknown	**UDDC = 1**	
NNNU = 28	**Unk; *n* = *7***	TCN1	Vitamin B transport
KIFC1	Cell cycle; M	**NDCD = 1**	
CHC1	Cell cycle; G2/M	AGR2	Cell survival
RPA2	Cell cycle; DNA damage	**NUCU = 1**	
MCM6	Cell cycle; S	FLJ1472	Unknown
CTH	Cysteine synthesis	**UUCD = 1**	

Table 1 Continued

Symbol	Function	Symbol	Function
CALD1	Cytoskeleton	SFRP2	WNT signaling
NASP	Histone transport	UDNN = 1	
COL2A1	ECM component	IL8RB	Immune response
LAMA1	ECM component	DCDC = 1	
DAG1	ECM component	KRT5	Cytoskeleton
P2RY2	Neuronal differentiation	NDCC; DNNN; NDCN	
NUP107	Nuclear transport	NDNN; NNDD; NNDN	
ANP32E	Phosphatase inhibitor	Unk; $n = 1$	

Each column contains highlighted categories that describe gene expression patterns on days 1, 3, 5, and 7 days post-amputation compared to basal gene expression (d0). Gene symbols are found under each category.

selected based on technical and biological rationale. Technically, we wanted to validate genes that yielded a broad range of relative fold change estimates by microarray analysis and included both possible directions of differential expression. These genes also exhibited a range of hybridization intensity values; for example, the average intensity value of *hairy enhancer of split 1* ranked among the bottom 37% of all probe sets while *galectin 1* (*lgals1*) ranked among the top 95%. Biologically, we selected genes that are of interest in regenerative biology and spinal cord injury research fields. A BioRad iScript cDNA synthesis kit (Hercules, CA, USA) was used to synthesize cDNA templates from three d0 and d3 RNA samples from microarray analysis. Primers were designed with Primer3 (Rozen and Skaletsky 2000) and used to amplify DNA fragments from the same gene regions that were used to design corresponding GeneChip probe sets (Table S3). Reactions included cDNA that was synthesized from 10 ng total RNA, 300 nmol/L primers, and iQ SYBR-Green real-time PCR mix (Bio-Rad, Hercules, CA, USA) and run on a Bio-Rad I Cycler QRT-PCR system (Bio-Rad). The three replicates were normalized against a gene that showed no significant gene expression change in the microarray experiment (glyceraldehyde-3-phosphate dehydrogenase, MC01187). PCR efficiencies for each primer were incorporated into the relative fold change calculations according to Pfaffl (2001). Student's *t*-tests were performed using the three normalized biological replicates for d0 and d3 samples.

In situ hybridization

Digoxygenin (DIG)-labeled RNA probe production and *in situ* hybridization (ISH) were performed as described by Hirota *et al.* (1992) with minor modifications. RNA probes were synthesized by *in vitro* transcription using 300–350 base pair PCR products as template and included SP6 or T3 RNA polymerase promoters appended to the 5′ ends (Table S3). PCR products were cleaned using Qiagen PCR purification columns (Qiagen, Valencia, CA, USA) before performing *in vitro* transcription. Axolotl tissues were collected three days after tail amputation and fixed at 4°C in 1× PBS, 4% paraformaldehyde overnight. Bone was decalcified by incubating the tissue in 500 mmol/L EDTA (pH8.0), 1× PBS for at least two days, cryoprotected overnight in 30% sucrose, and sectioned to 16 μm using a Microm 500 HM cryostat (Richard-Allan Scientific Inc., Kalamazoo, MI, USA). Hybridization, washing, and colorimetric detection with NBT/BCIP were performed on a Tecan Genesis Workstation 200 liquid handling robot with a Genepaint® hybridization station (Zurich, Switzerland). Microscopy was performed using an Olympus I X 81 microscope and images were acquired with an Olympus DP70 camera (Olympus, Center Valley, CA, USA).

Results

Histology of the spinal cord during the first week after tail amputation

We performed histology on tails collected 1, 3, 5, and 7 days after amputation to relate our experiment to previous morphological descriptions of urodele spinal cord and tail regeneration (Piatt 1955; Iten and Bryant 1976; Stensaas 1983). Upon amputation of the salamander tail, the spinal cord regresses approximately 0.5 mm rostral to the amputation plane and a clot, including a large number of leukocytes, forms at the wound site (Fig. 2a; Iten and Bryant 1976; Jones and Corwin 1993). By the end of the first week, the clot is replaced by a mesenchymous cell-mass called the blastema and the blastema forms while there is extensive extracellular matrix (ECM) remodeling and bone degeneration (arrows, Figs 2a, c, e and g). Also during the first several days, cell death occurs rostral to the injury plane and cell proliferation of inflammatory cells is apparent, but little cell division is observed among ependymal cells (Fig. 2b; Zhang *et al.* 2003; Stensaas 1983). By day 3, rostral axons begin to degenerate and ependymal cells migrate to close off the lumen of the spinal cord, thus creating a terminal bulb (Figs 2b, c, d and e; Egar and Singer 1972; data not shown). Ependyma become highly proliferative by day 7, increasing ependymal tube thickness and extending the tube along the length of the regenerating tail (Zhang *et al.* 2000). Following the first week of regeneration, ependymal cells differentiate into new CNS neurons and peripheral ganglia, reconnecting the spinal cord to the body periphery and recovering function (Koussoulakos *et al.* 1999).

Identification of differentially expressed genes and gene expression patterns

We identified 360 probe sets as detecting significantly different mRNA abundances between d0 and another time

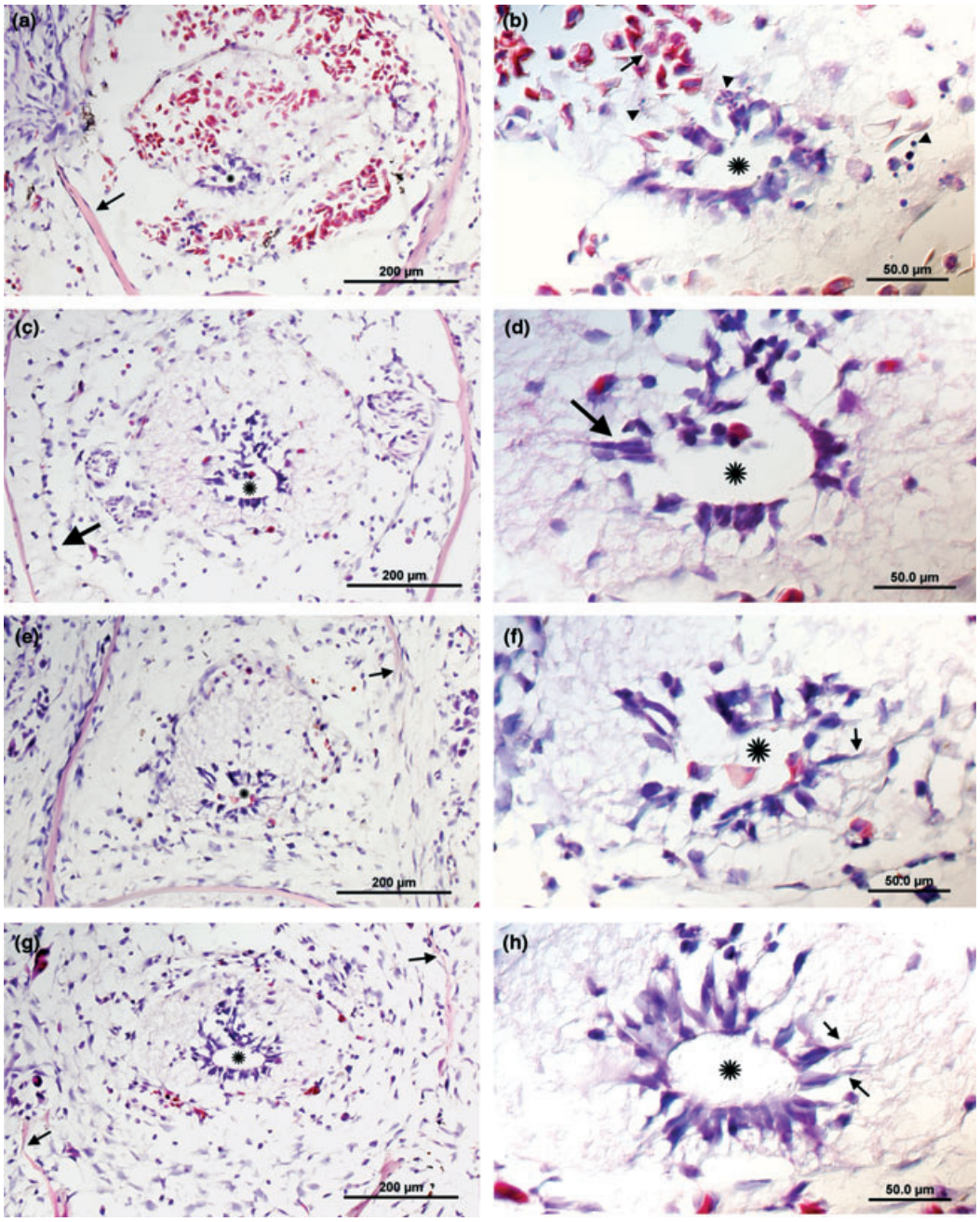

Fig. 2 Cross-sections of regenerating spinal cords at days 1 (a and b), 3 (c and d), 5 (e and f), and 7 (g and h) after tail amputation. Mayer's hematoxylin and eosin were used to stain chromatin blue and cytoplasm shades of red. Photographs were taken for sections within which the vertebrae were either fragmented or degenerating, and the central canal was clearly defined. (a and b) At day 1, hemorrhaging is apparent, the white matter degenerates, and there are few neurons within the spinal cord gray matter. Leukocytes and erythrocytes are present near the injury plane (stained deep red) with apoptotic bodies (arrowheads) near the loosely interconnected ependymoglial cells (blue cells surrounding central canal; star). Bone degeneration is minimal (a: arrow) and there is proliferation of leukocytes at the injury site (b: arrow). Bone degeneration increases throughout the first week (a, c, e and g: arrows). (e–h) A mesenchymous mass of cells (blastema) surrounds the regenerating spinal cord and ependymal cells project radial processes as the ependymal tube forms (d, f and h: arrows).

point (d1-7), using statistical and fold change thresholds (ANOVA $p < 0.01$; FWER of 0.01; $F_s > 28.36$; >2-fold). More than half of these probe sets ($n = 210$) correspond to salamander sequences (genes) that show high sequence identify to a presumptive human protein-coding locus; the remainder correspond to anonymous EST contigs. In com-

parison to d0 (baseline) mRNA levels, most genes exhibited significantly different mRNA abundances at two or more post-amputation time points. This temporal variability did not yield an extensive list of gene expression patterns. Although a total of 100 different gene expression patterns were possible under our scoring system, only 32 different patterns were observed and over 85% of all genes were classified into 10 categories (Table 1; Table S2). Eight of the top 10 categories identified groups of genes in which mRNA abundance increased or decreased at a particular time point, and afterward the level remained constant through d7. Transcript levels for a few genes did increase or decrease by >2-fold among post-amputation time points, however, only three genes (UNND) yielded a temporal expression profile that deviated significantly from baseline in both up- and down-regulated directions during the 7 day period (Table 1). Thus, the majority of the gene expression profiles that we examined consisted of a single, significant deviation from base line levels followed by relatively constant mRNA abundance. It is likely that many of the uniquely expressed genes at d7 are regulated at later time points because only 43 of the 360 genes exhibited transcript levels at d7 that approximated baseline. Clearly, we only sampled the initial phases of a continuous gene expression program that extends beyond d7. However, our experiment does precisely sample discrete phases of gene expression variability during this temporal process. For example, Fig. 3 illustrates that gene expression profiles of samples collected at d1 are much more similar to each other than samples collected at d0, as well as d3, 5, and 7. Below, we describe major gene expression patterns in greater detail. We also highlight some of the genes and gene functions that were found in each of the major gene expression categories. Finally, we compare the expression of salamander genes to presumptive rat orthologs that have been examined in microarray studies of spinal cord injury.

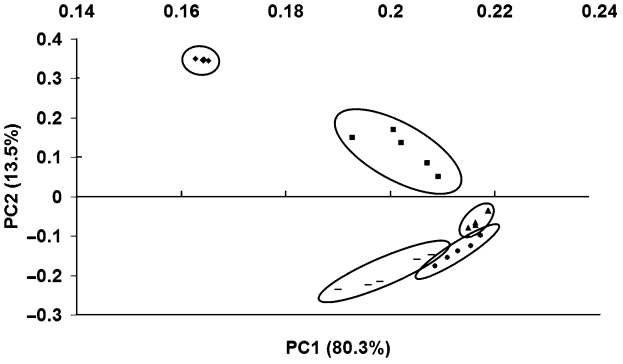

Fig. 3 Two-dimensional plot of a principal component analysis (PCA) showing the relatedness of each GeneChip. JMP statistical software was used to perform PCA on 25 GeneChips. A Pearson's correlation coefficient matrix was made for 25 GeneChips using intensity values for 376 changed genes. Principal component 1 (PC1; 80.35% of the variation; eigenvalue 20.09) is displayed on the *x*-axis and Principal component 2 (PC2; 13.54% of the variation; eigenvalue 3.34) is displayed on the *y*-axis. The cumulative variation accounted for by PC1 and PC2 is 93.89%. Twenty-five principal components account for 100% of the variation in the dataset. Five biological replicate Genechips used for each of the five time points are enclosed by an oval to illustrate their close proximity. ◆: d0, $n = 5$; ■: d1, $n = 5$; ▲: d3, $n = 5$; ●: d5, $n = 5$; –: d7, $n = 5$.

Gene expression patterns

Overall, a greater number of genes were up-regulated above baseline during the 7-day period ($n = 238$). The majority ($n = 134$) were significantly up-regulated at the first sample time after amputation (d1) and half of these genes (UCCC: $n = 64$) registered constant mRNA abundances above baseline at all subsequent post-amputation sample times (d3, d5, and d7). A substantial number of the d1 up-regulated genes showed decreasing mRNA abundances at later sample points. Some of these genes yielded mRNA abundances at d3 (UCNN: $n = 5$) or d5 (UCCN, UDNN: $n = 5$) that approximated d0 levels, while others remained above baseline (UDCC, UCDC, UNNU, UDDC: $n = 22$). The early group of up-regulated genes suggests that a diversity of regulatory pathways and biological processes are activated within the first 24 h after tail amputation. In addition to genes that presumably function in wounding, stress, inflammation, and immunity, this group includes genes that function in tissue remodeling, apoptosis, ion transport, cell–cell interactions, cell migration, vitamin B economy, lipid metabolism, and cytoskeleton dynamics (Table 1). Several different regulatory networks are implicated directly or indirectly among these d1 up-regulated responses, including MAPK, WNT, v-MYC, TNF, v-YES, RAS, and TGF-beta.

Other groups of genes were up-regulated for the first time at d3, 5, and 7 ($n = 104$). The majority of the d3 and d5 genes maintained high, constant mRNA levels at subsequent time points (NUCC: $n = 24$, NNUC: $n = 44$). Gene functions that were observed among d1 up-regulated genes were also represented among d3–7 up-regulated genes. However, the distribution of genes among these functional categories was very different. In particular, fewer injury response genes and a greater number of ECM and cytoskeleton-associated genes were observed compared to d1 up-regulated genes. Also, a greater number of cell cycle-related genes were observed (e.g., NNUC, cell cycle = 14), as well as genes that presumably function in DNA replication, metabolism, chromatin assembly, and cytokinesis. These results suggest that the regeneration gene expression program transitions during the first 7 days from an injury responsive phase to one that is defined primarily by the up-regulation of genes that function in cell division. Throughout both injury response and cell proliferation phases, genes that function in tissue remodeling are significantly regulated.

Relative to the total number of up-regulated genes, a much smaller number of genes ($n = 125$) were down-regulated

significantly below baseline levels during regeneration. In contrast to the up-regulated gene set, very few of these genes were down-regulated at d1 (DCCC, DCNN, DNNN, DCDC = 12). Also, the magnitude of the fold-level changes was generally lower than those measured for significantly up-regulated genes (mean of maximum up-regulated fold changes = 6.61; down-regulated = −3.07). The largest number of down-regulated genes was observed at d3 *(n* = 45) and this was followed by additional groups of down-regulated genes at d5 (n = 29) and d7 (n = 35). In general, many genes with neural related functions were down-regulated, including those that function in ion transport, glutamate metabolism, glutamate binding, neuroprotection, neurotransmission, neurogenesis, and lipid metabolism. Several functional categories that were observed among up-regulated genes were also observed among down-regulated genes, including apoptosis, cytoskeleton, ECM, signal transduction, and heat shock (Table 1). The overall pattern indicates that fewer genes are down-regulated during the first seven days of regeneration, and down-regulated genes show significantly lower mRNA abundances at d3, after the early up-regulation of genes at d1.

Some gene expression patterns were more complicated than linear, directional responses, involving changes in mRNA abundance that fluctuated both above and below the baseline. Some of these genes with complex expression patterns (UDCC, UCDC, NUCN, UDDC, NDCD, UUCD) may function in the regulation of biological processes during regeneration. These include genes that function in ECM remodeling (*matrix metalloproteinase [mmp] 1, mmp13, tissue inhibitor of metalloproteinase 1* [*timp1*]), coagulation (*tissue factor pathway inhibitor 2*), vitamin B transport (*intrinsic factor, transcobalamin 1*), cell proliferation (*v-Ha-ras viral oncogene, hypothetical protein FLJ20303*), transcriptional regulation (*jun-b proto-oncogene)*, and cell signaling (*latent TGF beta binding protein*; *chromosome 8 orf 4; secreted frizzled-related protein 2* [*sfrp2*]).

Gene expression after spinal cord injury: salamander verses rat

To identify similarities and differences between the salamander and mammalian spinal cord injury response, we compared our gene expression results to published results from the rat spinal cord microarray literature. Specifically, we compared the expression of 662 presumptive rat–salamander orthologous genes that are represented on both the *Ambystoma* and rat Affymetrix GeneChips. The resulting list of gene orthologs represents an unbiased sampling of ~24 000 transcripts on the rat arrays and 4590 transcripts on the salamander array. Although the majority of gene orthologs were not significantly regulated (n = 553), we identified many similar and dissimilar gene expression responses between these organisms. Eleven genes are up-regulated in both species, with no common genes down-regulated. There were 46 and 41 uniquely up-regulated genes in the salamander and rat, respectively. Overall, the majority of dissimilarities between the rat and salamander injury response were changes in one animal and not the other (n = 126) rather than opposite gene expression changes between animals (n = 2; Table S4).

Quantitative real-time PCR

Using QRT-PCR, we estimated fold change between d0 and d3 for 10 genes from the microarray experiment (Table 2). All of the transcripts that met statistical and fold level criteria from the microarray analysis registered significant differences in mRNA abundance by QRT-PCR (6/10). Overall, we were able to verify nine of the 10 gene changes in the correct direction with close agreement in most cases. We failed only to replicate the microarray estimate for *sox3*, which was not significant by QRT-PCR and registered such a low-fold change that it was excluded from the short list of microarray gene candidates. Thus, for all genes that met our stringent statistical and fold level criteria, and three genes that did not, QRT-PCR validated microarray estimates of gene expression with very good precision.

Spatial analysis of mRNAs using *in situ* hybridization

Ten genes that were significantly regulated during spinal cord regeneration were examined further by ISH. We probed tissues that were collected 3 days after tail amputation to localize expression among cell types that were within 1 mm from the end of the regenerating spinal cord. Figure 4 illustrates the diverse patterns of spatial expression observed with hybridization found in cells resembling ependymoglia, neurons, and immune cells. These results show that the general increase or decrease in mRNA abundance as determined from microarray analysis can be replicated and localized to specific cell populations and tissues of the spinal cord using ISH.

Table 2 Comparison of microarray versus real-time PCR estimates of fold change for ten genes that were quantified on d0 and d3

Sal ID	Gene name	Microarray	Real time
MC01620	SOX2	–1.7	–1.86**
MC02459	HES1	–2.15	–1.35
MC02501	SOX3	–1.92	1.14
MC03278	FST	3.09	3.45**
MC01765	CXCR4	3.17*	4.19**
MC01067	CD63	2.17*	4.77**
MC00341	TGFB1	3.69*	5.43**
MC01275	LGALS1	2.55*	10.5**
MC01583	SFRP2	17.95*	23.8**
MC03237	AGC1	56.84*	42.9**

*In the list of 360 genes that met statistical and fold level criteria.
**Significant fold change difference between d0 and d3 according to real-time PCR (student's unpaired *t*-test, $p < 0.05$).

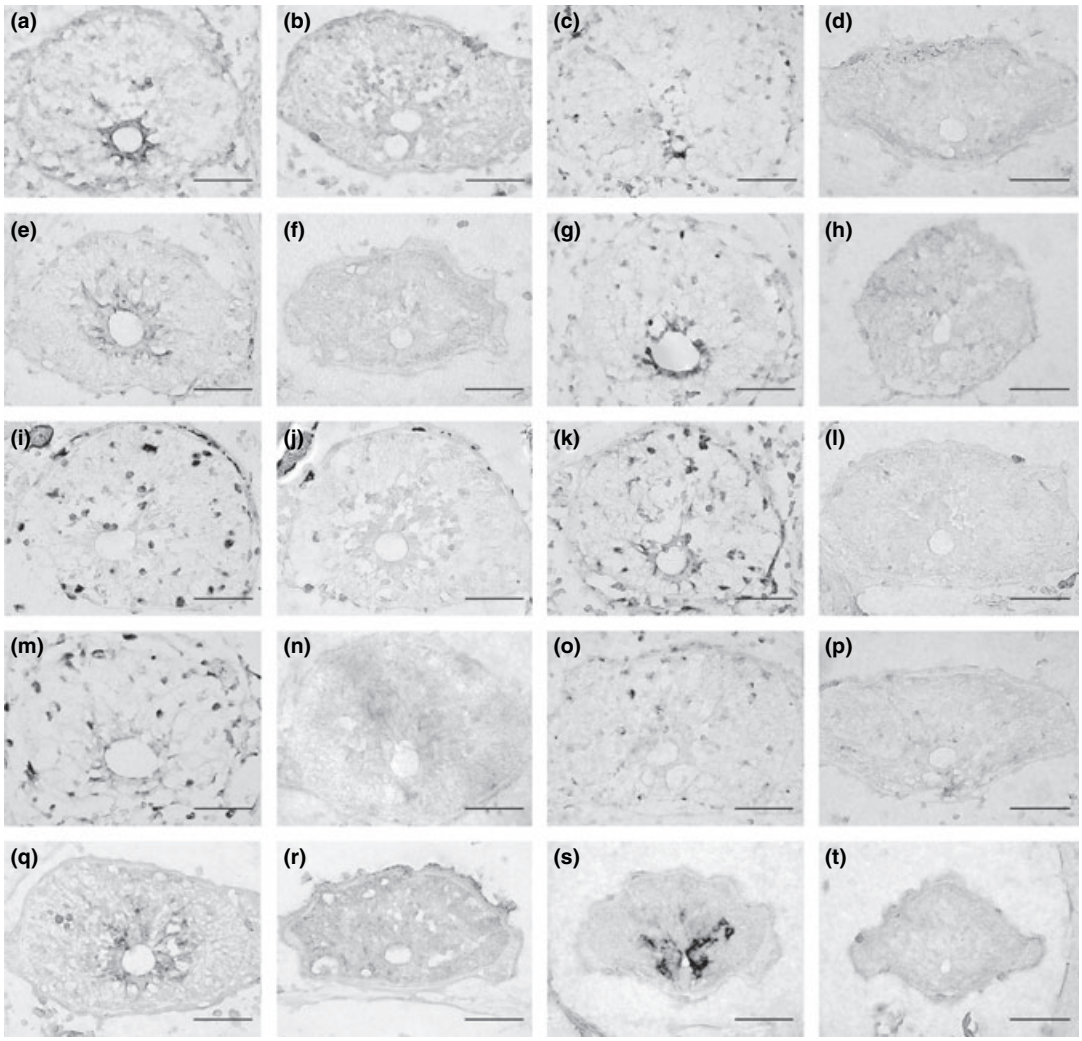

Fig. 4 *In situ* hybridizations of d3 (a–r) and d0 (s and t) axolotl spinal cords using DIG-RNA probes that correspond to significantly regulated genes from the microarray analysis. Anti-sense probes are represented in columns 1 and 3, and sense control probes in columns 2 and 4. *ck18* (a and b), *mmp9* (c and d), *Annexin A1* (e and f), and *sfrp2* (g and h) transcripts are all present in ependymal cells near the end of the regenerating spinal cord. Inflammatory-like cells that are found in the degenerating white matter are positive for *apoE* (i and j), *Ferritin-heavy polypeptide* (k and l), *lgals1* (m and n), and *lgals3* (o and p). *Thioredoxin* (q and r) transcripts are present in cells resembling ependyma, as well as neurons of the injured spinal cord. *Fibroblast growth factor binding protein 1* (s–t) is highly expressed in lateral ependyma and a subset of neurons in the uninjured spinal cord. Bar = 100 μm.

Discussion

We built a custom Affymetrix GeneChip and profiled gene expression during the early phases of natural spinal cord regeneration in a salamander model (*Ambystoma mexicanum*). Our results show that regeneration involves significant changes in mRNA abundance for many genes that are represented on the array. The overall list of 1273 genes that met a very stringent statistical criterion is available as a new resource for regeneration and spinal cord injury research fields (http://www.ambystoma.org). The large number of genes on this list, which were identified using a custom microarray with enriched gene content, shows that thousands of genes are significantly regulated during the first few days of natural spinal cord regeneration. We used additional statistical and fold change criteria to sample a smaller subgroup of candidate genes to describe gene expression patterns and biological functions. The presumptive functions of this smaller list of genes suggest the operation of many biological processes that change temporally during spinal cord regeneration. Below we discuss up-regulated and down-regulated genes and gene functions that may be important in the regenerative response. In particular, we compare our gene expression results to several studies that have examined rat spinal cord injuries using microarrays.

Up-regulated gene responses

Similar gene expression changes are often observed after tissue injury, regardless of the type of injury or specific tissue type examined. With respect to CNS tissue injury in mammals, an early acute phase is characterized in part by the expression of transcription factors and immune response genes. Our study identified several genes that change by d1 in salamander spinal cord that are also expressed during the mammalian CNS acute injury response (Bareyre and Schwab 2003; Vazquez-Chona *et al.* 2005). These include *jun-B proto-oncogene*, *interferon regulatory factor 1, heme oxygenase 1*, and *apolipoprotein E* (*apoE*). Overall, many of our d1 and d3 up-regulated genes encode proteins that participate in immune response functions, including lymphocyte, platelet and monocyte activation, macrophage differentiation and migration, cell adhesion, thrombosis, coagulation, inflammation, oxidative and metabolic stress, and apoptosis. In addition to immune response genes, we also observed up-regulation of genes that function in transport and binding of vitamin B and lipids, and ECM remodeling. Although processes like vitamin B homeostasis have received little attention in regeneration and injury fields (Bauer 1998), lipid turnover and MMP activity is well documented to be associated with regeneration (Vance *et al.* 2000; Vinarsky *et al.* 2005). In *A. mexicanum*, MMP1, MMP2, and MMP9 activity is associated with proliferating ependymal cells after 2–3 weeks of regeneration (Chernoff *et al.* 2000). Our study shows that *mmps 1*, *3*, *9*, *13*, *27*, and *timp1* are all highly up-regulated by 24 h after injury, which is the first association of *mmps 13* and *27* with regeneration in urodeles. MMPs are also up-regulated in rodents after SCI and high levels appears to contribute to secondary injury (Noble *et al.* 2002; Wells *et al.* 2003). Although application of MMP inhibitors may increase functional recovery after SCI, our results emphasize the beneficial effects of MMPs and the need to quantify the timing and amount of their delivery; clearly, MMP up-regulation and high MMP transcript levels after spinal cord amputation are characteristic of natural regeneration in *A. mexicanum*. In general, our results show a robust and diverse gene expression response is activated during the acute phase of natural spinal cord regeneration, and this response includes genes whose functions are thought deleterious to recovery after SCI in mammals.

The majority of the early-activated genes were up-regulated throughout the first seven days, extending into a subsequent phase of cell cycle-related gene expression at d5. The accumulation of mRNAs that increase during the first seven days of regeneration suggests a temporal change toward biological processes that are associated with cell division. Many genes up-regulated at d5 (NNUC) are associated with mitotic cell cycle regulation including four genes involved in the G2/M transition and six associated with mitosis (Table 1). These gene expression changes maybe associated with the early proliferation of blastemal and ependymal cell populations, which are known to expand after the first week of regeneration (Lo *et al.* 1993; Zhang *et al.* 2003). Cell cycle-related genes are also up-regulated early after rat spinal cord injury, but the functions of these genes are associated primarily with S-phase and DNA repair and expressed in damaged or apoptotic neurons, not proliferating cells (Di Giovanni *et al.* 2003). Thus, within a few days after spinal cord injury, cell-cycle gene expression is biased towards cell death pathways in mammals but cell survival and proliferation pathways in salamanders.

Down-regulated gene responses

In comparison to up-regulated genes, there were fewer down-regulated genes and most showed gradual changes over time. Multiple genes were down-regulated whose products are associated with neural functions, including axon guidance, ion transport, glutamate metabolism, neuroprotection, and neurotransmitter signaling. Changes in neural-related gene expression patterns may reflect the damage or loss of neural cell types verses the survival, infiltration, and proliferation of other cell types. This explanation has been advanced to explain the down-regulation of genes after mammalian spinal cord injury, where there can be extensive tissue damage and cell loss (Profyris *et al.* 2004). Indeed, even in the regenerating salamander, there is local spinal cord tissue loss after injury (Fig. 2b; Zhang *et al.* 2003; Stensaas 1983). Thus, in both mammals and salamanders, many of the down-regulated gene expression patterns may reflect the stochastic nature of cell survival at the injury site. However, we did observe significant down-regulation of several genes that are associated with glutamate metabolism and transport, that are up-regulated after CNS injury in mammals. This suggests the possibility that some genes are actively and uniquely repressed during salamander regeneration.

Identification of genes expressed differently between salamander regeneration and rat spinal cord injury

We compared genes that changed during early salamander spinal cord regeneration to gene lists that were compiled from microarray studies of spinal cord injury in rats. We acknowledge that this comparison is potentially confounded by several sources of variation including experimental, technical, statistical, tissue, and organismal differences. However, as we described above, some of the same genes that are expressed early after mammalian CNS injury are also up-regulated during spinal cord regeneration in salamander. If similar gene expression programs underlie homologous tissues, then comparisons of homologous tissues among distantly related organisms may filter conserved gene expression responses and help identify uniquely regulated genes. Some of the uniquely regulated genes from salamander are associated with regeneration in other organisms and tissues including amphibian limb regeneration (*cytokeratin 18* [*ck18*], Corcoran and Ferretti 1997; *msx1*, Beck *et al.*

2003*; msx2*, Carlson *et al.* 1998; and *mmp9*, Yang *et al.* 1999), fish tailfin regeneration (*ck18* and *periostin*, Padhi *et al.* 2004), and annelid epimorphic regeneration (*phosphoribosylaminoimidazole carboxylase*, Myohara *et al.* 2006). Several other up-regulated genes are associated with mammalian liver regeneration, including *follistatin* (*fst*; Borgnon *et al.* 2005), *cystathionase* (Teshigawara *et al.* 1995), *laminin alpha 1* (Kikkawa *et al.* 2005), *transglutaminase 1* (Ohtake *et al.* 2006), and *uncoupling protein 2* (Horimoto *et al.* 2004). Furthermore, eight cell cycle genes, a necessary process for true tissue regeneration, are present within this unique salamander gene list including *cell division cycle 2*, *kinesin family member 11*, and *mitotic arrest deficient-like 1*. Up-regulation of the same gene orthologs across multiple regeneration paradigms suggests that regeneration is definable across taxa and tissues by distinct gene expression patterns. Further studies are needed to determine if a conserved group of genes function in molecular pathways that are required for regeneration.

Molecules that regulate morphogenic signaling

Morphogenic molecules, such as sonic hedgehog (SHH), bone morphogenic proteins (BMPs), WNT factors, and fibroblast growth factors (FGFs) have been associated with regeneration because they establish positional identity, control cell proliferation, and regulate cell fate during development (Schnapp *et al.* 2005; Vergara *et al.* 2005; Whitehead *et al.* 2005; Niemann 2006). In this study, we identified changed genes that code for extracellular molecules that participate in BMP, WNT, and FGF signaling. *fst* encodes a protein that regulates dorsal–ventral patterning of the developing vertebrate CNS through BMP inhibition and is up-regulated during the first week of regeneration (Table 2; NUCC; Lee and Jessell 1999). mRNAs for *sfrp2*, a secreted WNT antagonist that blocks ligand binding to frizzled receptors (Kawano and Kypta 2003), is also highly up-regulated (Table 2; UUCD; Fig. 4g-h). Furthermore, *wnt5A* demonstrates a 3.86-fold increase in expression (UCCC), suggesting a network of pro- and negative WNT signaling during regeneration. Lastly, *fibroblast growth factor binding protein 1*, a secreted molecule that sequesters FGF ligands from the ECM (Tassi *et al.* 2001) is down-regulated 6.42-fold at 24 h (DCCC; Figs 4s–t). These large gene expression changes suggest that BMP, WNT, and FGF signaling pathways are all altered during early spinal cord regeneration. Further studies with each of these molecules and their corresponding binding substrates will be needed in order to assess their possible roles during regeneration.

Conclusion

The salamander's unique ability to regenerate complex body parts has long been recognized as an important model in developmental biology, however, salamanders have received relatively little attention from researchers of mammalian spinal cord injury. Our study shows that genomic and bioinformatics resources are now available to associate gene expression changes with cellular and molecular aspects of natural spinal cord regeneration. The emerging salamander perspective on regeneration promises to extend existing research paradigms and may suggest novel therapies for CNS injury in humans.

Acknowledgements

The project described was supported by the Kentucky Spinal Cord Injury Research Trust and Grant Number 5-R24-RR016344-06 from the National Center for Research Resources (NCRR), a component of the National Institutes of Health (NIH). Its contents are solely the responsibility of the authors and do not necessarily represent the official views of NCRR or NIH. We thank Jeramiah Smith for help in designing the *Ambystoma* GeneChip and comments and suggestions throughout the project.

Supplementary material

The following material is available for this paper online

Table S1. Gene list for 360 changed genes with functions and fold changes relative to day 0.

Table S2. Distribution of gene expression patterns for 360 significantly regulated salamander genes during spinal cord regeneration.

Table S3. Primer sequences for QRT-PCR and *in situ* hybridization analysis.

Table S4. Gene list for changed genes found on both the *Ambystoma* and rat U34 Affymetrix GeneChips.

This material is available as part of the online article from http://www.blackwell-synergy.com

Please note: Blackwell Publishing are not responsible for the content or functionality of any supplementary materials supplied by the authors. Any queries (other than missing material) should be directed to the corresponding author for the article.

References

Aimone J. B., Leasure J. L., Perreau V. M. and Thallmair M. (2004) Spatial and temporal gene expression profiling of the contused rat spinal cord. The Christopher Reeve Paralysis Foundation Research Consortium. *Exp. Neurol.* **189**, 204–211.

Bareyre F. M. and Schwab M. E. (2003) Inflammation, degeneration and regeneration in the injured spinal cord: insights from DNA microarrays. *Trends Neurosci.* **26**, 555–563.

Bauer J. A. (1998) Hydroxocobalamins as biologically compatible donors of nitric oxide implicated in the acceleration of wound healing. *Med. Hypotheses* **51**, 65–67.

Beck C. W., Christen B. and Slack J. M. (2003) Molecular pathways needed for regeneration of spinal cord and muscle in a vertebrate. *Dev. Cell* **5**, 429–439.

Benjamini Y. and Hochberg Y. (1995) Controlling the false discovery rate: a practical and powerful approach to multiple testing. *J. Royal Stat. Soc. Ser. B* **57**, 289–300.

Bolstad B., Irizarry R., Gautier L. and Wu Z. (2005a) Preprocessing high-density oligonucleotide arrays, in *Bioinformatics and Computational Biology Solutions Using R and Bioconductor* (Gentleman R., Carey V., Huber W., Irizarry R. and Dudoit S., eds.), pp. 13–32. Springer, New York.

Bolstad B., Collin F., Brettschneider J., Simpson K., Cope L., Irizarry R. A. and Speed T. P. (2005b) Quality assessment of Affymetrix GeneChip data, in *Bioinformatics and Computational Biology Solutions Using R and Bioconductor* (Gentleman R., Carey V., Huber W., Irizarry R. and Dudoit S., eds.), pp. 33–47. Springer, New York.

Borgnon J., Djamouri F., Lorand I., Rico V. D., Loux N., Pages J. C., Franco D., Capron F. and Weber A. (2005) Follistatin allows efficient retroviral-mediated gene transfer into rat liver. *Biochem. Biophys. Res. Commun.* **328**, 937.

Carlson M. R., Bryant S. V. and Gardiner D. M. (1998) Expression of Msx-2 during development, regeneration, and wound healing in axolotl limbs. *J. Exp. Zool.* **282**, 715–723.

Carlson M. R. J., Komine Y., Bryant S. V. and Gardiner D. M. (2001) Expression of Hoxb13 and Hoxc10 in developing and regenerating axolotl limbs and tails. *Dev. Biol.* **229**, 396–406.

Carmel J. B., Galante A., Soteropoulos P., Tolias P., Recce M., Young W. and Hart R. P. (2001) Gene expression profiling of acute spinal cord injury reveals spreading inflammatory signals and neuron loss. *Physiol. Genomics* **7**, 201–213.

Caubit X., Nicolas S. and Le Parco Y. (1997) Possible roles for Wnt genes in growth and axial patterning during regeneration of the tail in urodele amphibians. *Dev. Dyn.* **210**, 1–10.

Chernoff E. A., O'Hara C. M., Bauerle D. and Bowling M. (2000) Matrix metalloproteinase production in regenerating axolotl spinal cord. *Wound Repair and Regeneration* **8**, 282–291.

Choe S. E., Boutros M., Michelson A. M., Church G. M. and Halfon M. S. (2005) Preferred analysis methods for Affymetrix GeneChips revealed by a wholly defined control dataset. *Genome Biol.* **6**, R16.

Christensen R. N., Weinstein M. and Tassava R. A. (2002) Expression of fibroblast growth factors 4, 8, and 10 in limbs, flanks, and blastemas of Ambystoma. *Dev. Dyn.* **223**, 193–203.

Corcoran J. P. and Ferretti P. (1997) Keratin 8 and 18 expression in mesenchymal progenitor cells of regenerating limbs is associated with cell proliferation and differentiation. *Dev. Dyn.* **210**, 355–370.

Cui X., Hwang J. T., Qiu J., Blades N. J. and Churchill G. A. (2005) Improved statistical tests for differential gene expression by shrinking variance components estimates. *Biostatistics* **6**, 59–75.

De Biase A., Knoblach S. M., Di Giovanni S., Fan C., Molon A., Hoffman E. P. and Faden A. I. (2005) Gene expression profiling of experimental traumatic spinal cord injury as a function of distance from impact site and injury severity. *Physiol. Genomics* **22**, 368–381.

Di Giovanni S., Knoblach S. M., Brandoli C., Aden S. A., Hoffman E. P. and Faden A. I. (2003) Gene profiling in spinal cord injury shows role of cell cycle in neuronal death. *Ann. Neurol.* **53**, 454–468.

Draghici S., Khatri P., Eklund A. C. and Szallasi Z. (2006) Reliability and reproducibility issues in DNA microarray measurements. *Trends Genet.* **22**, 101–109.

Egar M. and Singer M. (1972) The role of ependyma in spinal cord regeneration in the urodele, *Titurus*. *Exp. Neurol.* **37**, 422–430.

Hay E. and Fischman D. (1961) Origin of the blastema in regenerating limbs of the newt Triturus viridescens. An autoradiographic study using tritiated thymidine to follow cell proliferation and migration. *Dev. Biol.* **3**, 26–59.

Hirota S., Ito A., Morii E., Wanaka A., Tohyama M., Kitamura Y. and Nomura S. (1992) Localization of mRNA for c-kit receptor and its ligand in the brain of adult rats: an analysis using in situ hybridization histochemistry. *Brain Res. Mol. Brain Res.* **1**, 47–54.

Horimoto M., Fulop P., Derdak Z., Wands J. R. and Baffy G. (2004) Uncoupling protein-2 deficiency promotes oxidant stress and delays liver regeneration in mice. *Hepatology* **39**, 386–392.

Irizarry R. A., Hobbs B., Collin F., Beazer-Barclay Y. D., Antonellis K. J., Scherf U. and Speed T. P. (2003) Exploration, normalization, and summaries of high density oligonucleotide array probe level data. *Biostatistics* **4**, 249–264.

Iten L. E. and Bryant S. V. (1976) Stages of tail regeneration in the adult newt, *Notophthalmus viridescens*. *J. Exp. Zool.* **196**, 283–292.

Jones J. and Corwin J. (1993) Replacement of lateral line sensory organs during tail regeneration in salamanders: Identification of progenitor cells and analysis of leukocyte activity. *J. Neurosci.* **13**, 1022–1034.

Kawano Y. and Kypta R. (2003) Secreted antagonists of the Wnt signaling pathway. *J. Cell Sci.* **116**, 2627–2634.

Kikkawa Y., Mochizuki Y., Miner J. H. and Mitaka T. (2005) Transient expression of laminin alpha1 chain in regenerating murine liver: restricted localization of laminin chains and nidogen-1. *Exp. Cell Res.* **305**, 99–109.

Koussoulakos S., Margaritis L. H. and Anton H. J. (1999) Origin of renewed spinal ganglia during tail regeneration in urodeles. *Dev. Neurosci.* **21**, 134–139.

Lee K. J. and Jessell T. M. (1999) The specification of dorsal cell fates in the vertebrate central nervous system. *Ann. Rev. of Neurosci.* **22**, 261–294.

Lo D. C., Allen F. and Brockes J. P. (1993) Reversal of muscle differentiation during urodele limb regeneration. *PNAS* **90**, 7230–7234.

Millenaar F. F., Okyere J., May S. T., van Zanten M., Voesenek L. A. and Peeters A. J. (2006) How to decide? Different methods of calculating gene expression from short oligonucleotide array data will give different results. *BMC Bioinformatics* **7**, 137.

Müller H. (1864) Ueber regeneration der wirbelsäule und des rückenmarks bei Tritonen und Eidechsen. *Abhandl. d. Senckenbergischen nature-forsch. Gesellsch* **5**, 113–136.

Myohara M., Niva C. C. and Lee J. M. (2006) Molecular approach to annelid regeneration: cDNA subtraction cloning reveals various novel genes that are upregulated during the large-scale regeneration of the oligochaete, *Enchytraeus japonensis*. *Dev. Dyn.* **235**, 2051–2070.

Niemann C. (2006) Controlling the stem cell niche: right time, right place, right strength. *BioEssays* **28**, 1–5.

Noble L. J., Donovan F., Igarashi T., Goussev S. and Werb Z. (2002) Matrix metalloproteinases limit functional recovery after spinal cord injury by modulation of early vascular events. *J. Neurosci.* **22**, 7526–7535.

Nordlander R. H. and Singer M. (1978) The role of ependyma in regeneration of the spinal cord in the urodele amphibian tail. *J. Comp. Neur.* **180**, 349–374.

O'Hara C. M. and Chernoff E. A. (1994) Growth factor modulation of injury-reactive ependymal cell proliferation and migration. *Tissue Cell* **26**, 599–611.

Ohtake Y., Maruko A., Abe S., Fukumoto M. and Ohkubo Y. (2006) Effect of retinoic acid-induced transglutaminase on cell growth in regenerating liver. *Biomed. Res.* **27**, 75–80.

Padhi B. K., Joly L., Tellis P., Smith A., Nanjappa P., Chevrette M., Ekker M. and Akimenko M. A. (2004) Screen for genes differentially expressed during regeneration of the zebrafish caudal fin. *Dev. Dyn.* **231**, 527–541.

Page R. B., Monaghan J. R., Samuels A. K., Smith J. J., Beachy C. K. and Voss S. R. (2006) Microarray analysis identifies keratin loci as sensitive biomarkers for thyroid hormone disruption in salamanders (*Ambystoma*). *Comp. Biochem. Physiol. Part C* doi:10.1016/j.cbpc.2006.06.003.

Pfaffl M. W. (2001) A new mathematical model for relative quantification in real-time RT-PCR. *Nucl. Acids Res.* **29**, e45.

Piatt J. (1955) Regeneration of the spinal cord in the salamander. *J. Exp. Zool.* **129**, 177–207.

Profyris C., Cheema S. S., Zang D., Azari M. F., Boyle K. and Petratos S. (2004) Degenerative and regenerative mechanisms governing spinal cord injury. *Neurobiol. Dis.* **15**, 415–436.

Putta S., Smith J. J., Walker J. A. *et al.* (2004) From biomedicine to natural history research: EST resources for ambystomatid salamanders. *BMC Genomics* **5**, 54.

Rozen S. and Skaletsky H. (2000) Primer3 on the WWW for general users and for biologist programmers, in *Bioinformatics Methods and Protocols: Methods in Molecular Biology* (Krawetz S. and Misener S., eds.), pp. 365–386. Humana Press, Totowa, NJ.

Schnapp E., Kragl M., Rubin L. and Tanaka E. M. (2005) Hedgehog signaling controls dorsoventral patterning, blastema cell proliferation and cartilage induction during axolotl tail regeneration. *Development* **132**, 3243–3253.

Song G., Cechvala C., Resnick D. K., Dempsey R. J. and Rao V. L. (2001) GeneChip® analysis after acute spinal cord injury in rat. *J. Neurochem.* **79**, 804–815.

Spallanzani L. (1769) Prodromo di un opera da imprimersi sopra la riproduzioni animal: (An essay on animal reproduction), in Mati M. translation. T. Becket and de Hondt, London.

Stensaas L. J. (1983) Regeneration in the spinal cord of the newt *Notopthalmus* (Titurus) *pyrrhogaster*, in *Spinal Cord Reconstruction* (Kao C. C. and Reier P. J., eds.), pp. 121–150. Raven Press, New York.

Tassi E., Al-Attar A., Aigner A., Swift M. R., McDonnell K., Karavanov A. and Wellstein A. (2001) Enhancement of fibroblast growth factor (FGF) activity by an FGF-binding protein. *J. Biol. Chem.* **276**, 40 247–40 253.

Teshigawara M., Matsumoto S., Tsuboi S. and Ohmori S. (1995) Changes in levels of glutathione and related compounds and activities of glutathione-related enzymes during rat liver regeneration. *Res. Exp. Med. (Berl)* **195**, 55–60.

Torok M. A., Gardiner D. M., Izpisua-Belmonte J. C. and Bryant S. V. (1999) Sonic Hedgehog (shh) expression in developing and regenerating axolotl limbs. *J. Exp. Zool.* **284**, 197–206.

Tsai J., Sultana R., Lee Y., Pertea G., Karamycheva S., Antonescu V., Cho J., Parvizi B., Cheung F. and Quackenbush J. (2001) RESOURCERER: a database for annotating and linking microarray resources within and across species. *Genome Biol.* **2**, software0002.1–0002.4.

Vance J. E., Campenot R. B. and Vance D. E. (2000) The synthesis and transport of lipids for axonal growth and nerve regeneration. *Biochim. Biophys. Acta* **1486**, 84–96.

Vazquez-Chona F. R., Khan A. N., Chan C. K. *et al.* (2005) Genetic networks controlling retinal injury. *Mol. Vis.* **11**, 958–970.

Vergara M. N., Arsenijevic Y. and Del Rio-Tsonis K. (2005) CNS regeneration: a morphogen's tale. *J. Neurobiol.* **64**, 491–507.

Vinarsky V., Atkinson D. L., Stevenson T. J., Keating M. T. and Odelberg S. J. (2005) Normal newt limb regeneration requires matrix metalloproteinase function. *Dev. Biol.* **279**, 86–98.

Wells J. E. A., Rice T. K., Nuttall R. K., Edwards D. R., Zekki H. and Rivest S. (2003) An adverse role for matrix metalloproteinase 12 after spinal cord injury in mice. *J. Neurosci.* **23**, 10 107–10 115.

Whitehead G. G., Makino S., Lien C. L. and Keating M. T. (2005) fgf20 Is Essential for Initiating Zebrafish Fin Regeneration. *Science* **310**, 1957–1960.

Yang E. V., Gardiner D. M., Carlson M. R., Nugas C. A. and Bryant S. V. (1999) Expression of Mmp-9 and related matrix metalloproteinase genes during axolotl limb regeneration. *Dev. Dyn.* **216**, 2–9.

Zhang F., Clarke J. and Ferretti P. (2000) FGF-2 Up-regulation and proliferation of neural progenitors in the regenerating amphibian spinal cord *in vivo*. *Dev. Biol.* **225**, 381–391.

Zhang F., Clarke J., Santos-Ruiz L. and Ferretti P. (2002) Differential regulation of fibroblast growth factor receptors in the regenerating amphibian spinal cord *in vivo*. *Neuroscience* **114**, 837–848.

Zhang F., Ferretti P. and Clarke J. (2003) Recruitment of postmitotic neurons into the regenerating spinal cord of urodeles. *Dev. Dyn.* **226**, 341–348.

